## PROCEEDINGS OF SPIE

SPIEDigitalLibrary.org/conference-proceedings-of-spie

# Design, fabrication, and characterization of dielectric elastomer actuator enabled cuff compression device

Venkatraman, Rahul, Kaaya, Theophilus, Tchipoque, Helio, Cluff, Kim, Asmatulu, Ramazan, et al.

Rahul J. Venkatraman, Theophilus Kaaya, Helio Tchipoque, Kim Cluff, Ramazan Asmatulu, Ryan Amick, Zheng Chen, "Design, fabrication, and characterization of dielectric elastomer actuator enabled cuff compression device," Proc. SPIE 12042, Electroactive Polymer Actuators and Devices (EAPAD) XXIV, 1204205 (20 April 2022); doi: 10.1117/12.2613250



Event: SPIE Smart Structures + Nondestructive Evaluation, 2022, Long Beach, California, United States

### Design, Fabrication, and Characterization of Dielectric Elastomer Actuator Enabled Cuff Compression Device

Rahul J. Venkatraman<sup>a</sup>, Theophilus Kaaya<sup>a</sup>, Helio Tchipoque<sup>a</sup>, Kim Cluff<sup>b</sup>, Ramazan Asmatulu<sup>b</sup>, Ryan Amick<sup>b</sup>, and Zheng Chen<sup>a</sup>

<sup>a</sup>University of Houston, 4800 Calhoun Rd, Houston, TX 77004, USA <sup>b</sup>Wichita State University, 1845 Fairmount St, Wichita, Kansas, KS 67260, USA

#### ABSTRACT

Wearable dielectric elastomer actuators (DEAs) have been greatly considered for development of biomedical devices. In particular, a DEA cuff device has the capability of minimizing venous system disorders that occur in the lower limbs such as orthostatic intolerance (OI) and deep-vein thrombosis which are a result of substantial blood pooling. Recent works have shown that DEAs could regulate and even enhance venous blood flow return. This wearable technology offers a new light, low-cost, compliant, and simple countermeasure which could be safely and comfortably worn that includes mobility. In addition, it may supplement or even provide an alternative solution to exercise and medication. This work presents the design, model, and characterization of the DEA cuff device design that is capable of generating significant pressure change. A rolled DEA strip was actuated over a simulated muscle-artery apparatus using periodic a voltage input, and fluid pressure change was directly observed. A force sensitive resistor sensor was used to achieve a more precise pressure measurement. Performance analysis was conducted through frequency response analysis. The results provide a framework for implementing dynamic modelling and control to allow various forms of actuation input.

Keywords: Dielectric elastomer actuators, soft actuators, wearable devices, compression devices, spaceflight countermeasure

#### 1. INTRODUCTION

The circulatory system, which is responsible for the movement blood to and from the heart through arteries and veins, supplies oxygen and other nutrients to muscles, connective tissue, organs, and other cellular structures. The stroke volume (SV) is the amount of blood that is ejected from the heart.<sup>2</sup> The muscular system depends on oxygen and nutrients carried by the blood to function properly. These essentials are delivered to muscles for growth and recovery during rest. Muscles specifically in the lower limbs can demand little to large amounts of oxygen depending on magnitude of the physical activity. Cardiovascular strength is continuously used to overcome gravitational forces during physical activity and for adapting to body orientations including being in a standing position. Gravitational effects are essential during postural changes, notably in controlling any venous blood pooling.<sup>3</sup> Blood circulation challenges can lead to cardiovascular diseases and muscle atrophies that commonly originate from many different sources including genetics related to family health history, recovery and rehabilitation from injuries or surgical procedures. Such challenges are also a result of occupation where the human body undergoes dynamic, intense, or prolonged changes that have direct impact on blood flow. Athletes conduct aerobic and anaerobic activities which demand high amounts of oxygen and nutrients to be transported to muscles to perform at the highest capacity. Insufficient blood transport prevents involuntary or voluntary contracted muscles from relaxing leading to claudication, (also known as muscle pain), cramps, spasms, strains, and tears. Progression of age leads to more chronic and severe cases typically from cardiovascular diseases. Astronauts experience similar consequences in spaceflight and upon arrival on Earth. The reduction of gravitational forces reduces SV leading to a reduction of muscle mass. The changes that astronauts experience in space are analogous to natural aging process of the human body on Earth. Orthostatic intolerance (OI) is the

Further author information: (Send correspondence to Z. Chen) Z.Chen: E-mail: zchen43@Central.uh.edu, Telephone:+1-713-743-6427

Electroactive Polymer Actuators and Devices (EAPAD) XXIV, edited by Iain A. Anderson John D. W. Madden, Herbert R. Shea, Proc. of SPIE Vol. 12042, 1204205 © 2022 SPIE · 0277-786X · doi: 10.1117/12.2613250

inability for adapting and maintaining blood pressure while standing.<sup>6</sup> The human body can undergo a painful process, especially in the lower limbs to overcome OI even with post-flight rehabilitation.

The development of a cuff device could offer both a preventive and proactive tool as well as a rehabilitation tool to regulate and enhance blood flow (Figure 1). The novelty of such a devices lies in the mechanics, materials, and control system used to develop a robust design. Previous work highlighted below has demonstrated that





Figure 1: Design concept for a light-weight and portable DEA cuff worn over the thigh.

DEA enabled compression devices provide a low-cost, lightweight, and portable solution that is compliant for generating pressure change to regulate and enhance blood flow in the lower limbs. DEAs are lightweight and flexible materials that deform in response to an electrical input. Their electromechanical properties make DEAs attractive for biomorphic robots. DEAs behave in a restoring manner in which applying voltage across the membrane results into deformation in all directions and removing voltage restores the membrane to the original shape. Materials required to develop DEAs can facilitate movement that mimic human muscles simpler than electrically driven motors as shown in modelling and control of a DE diaphragm actuator. DEAs are capable of generating contraction forces as strong as natural muscles. The motivation described earlier calls for DEAs to produce pressure change. This can be achieved by stacking or, in this case, rolling multiple layers of DE material. Generating a macro-sized change using rolled or stacked actuators can require hundreds of layers as documented in a paper showing 0.16N/mm<sup>2</sup> of actuation pressure for a stack actuator.<sup>10</sup> An active compression bandage (ACB), that was fabricated with DEAs, reported a pressure change of 5.2% for a single layer actuated at 11.3 kV, and an analytical model was simulated to show a pressure change of 8.0% for three layers. 11 This work demonstrated the influence of electrical input and elastomer geometry, to pressure change through constant actuation. A DEA-spring design that was also utilized for active compression reported a pressure change of 2.55mm Hg (340 Pa) with a starting pressure of 26mm Hg (3466.38 Pa) when constantly actuated at 1.2 kV.  $^{12}$ It is worth noting that the net blood pressure in a healthy individual, that is the difference in systolic and diastolic blood pressures (120/80), is 40 mm Hg (5333 Pa), and so where the unactuated (maximum) pressure and actuated (minimum) pressure is set is a critical element to performance. This paper investigates the feasibility of providing dynamic actuation through periodic(or cyclic) actuation. In other words, rather than providing constant actuation, pressure can be regulated based on actuation frequency. This paper is structured as follows: Section 2 discusses the design and fabrication of the DEA Cuff, section 3 discusses the experimental and model validation, and section 4 the conclusion and future work.

#### 2. DESIGN AND FABRICATION OF DEA CUFF

In this section the design of the DEA cuff is presented as well as its fabrication and application.

#### 2.1 Designing DEA Cuff

For this design, a DEA strip is rolled over a compression sleeve two times (Figure 2). Increasing the number of layers increases the number of roll turns thereby amplifying the force output. <sup>13</sup> One end of the DEA strip is kept fixed on the compression sleeve, and then rolled over. In this case, force does not increase with applied voltage, but rather decreases as the elastomer expands radially. The multi-layer DEA strip along with the compression sleeve increase pressure to the artery. The fluctuating voltage, from 0 V to the desired input, results in the periodic change between applied pressure and released pressure. Applied pressure reduces blood flow and released pressure increases it.

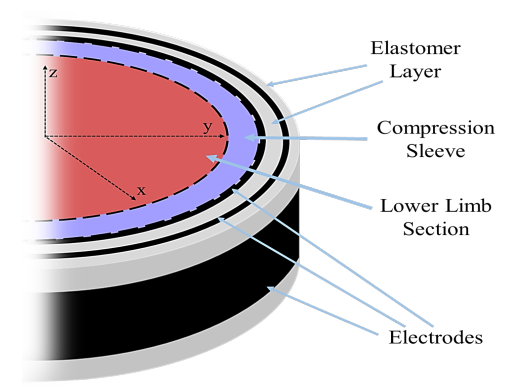


Figure 2: Cross-section of the DEA Cuff.

A thin compression sleeve makes up the inner most layer of the DEA Cuff. This layer acts a thermal and insulating barrier to prevent any electrical contact between electrodes and the skin of the lower-limb section. The thin material also allows minimal resistance to motion provided by the actuator. Following the compression layer is the two-layer rolled actuator which comprises of the elastomer and painted electrodes. A static-based physical model to show total pressure of a DEA compression device has been derived in work done by Pourazadi et al, <sup>11</sup> and the basis for developing a dynamic-based model is shown in work by Kaaya et al. <sup>14</sup> The process for applying the DEA layer and compression sleeve is further explained in section 2.2.

#### 2.2 DEA Fabrication and Application

The DEA strip was fabricated using 3M very high bond (VHB) 4910 tape as the elastic membrane. A 30 cm x 6.5 cm DEA strip was cut for this experiment (Figure 3a). A border was measured at 1.5 cm into each side of the elastomer for creating the painted region for electrode application. The red VHB protective layer was applied on the border to make electrode application easier. Carbon powder (99.5% graphite powder, CAS# 7782-42-5), chosen as the electrode, was painted within the border. The border was then removed and used to measure a small painting region that extended from the electrode area. A copper tape strip was cut and placed on the small painted region. Careful painting was required in order to avoid short circuit or electric contact with any other adjoining components. The painted membrane was turned over, and the painting process and lead attachment was repeated. The two opposite leads provide the positive and negative connections to the power supply.

The DEA Cuff was fitted on a 1:2.25 scaled-down calf section. The scale-down factor was based on the limited 3d printing space for the calf mold. Ecoflex 00-30 two-part mixture silicone rubber was used to roughly approximate the elastic stiffness of the calf muscle. Generous amounts of silicone mixture was poured and cured in a 3d printed mold. After curing, the silicone muscle was removed and further aired out to ensure a solidity. A plastic tube containing sugar water was used to mimic the artery. A tiny hole was pierced, and the excess fluid poured into a cup. This tiny piercing was made such that a flexible rubber tube can be inserted and glued to the plastic tube. This tube represents a superficial capillary that is utilized for observable fluid pressure change.

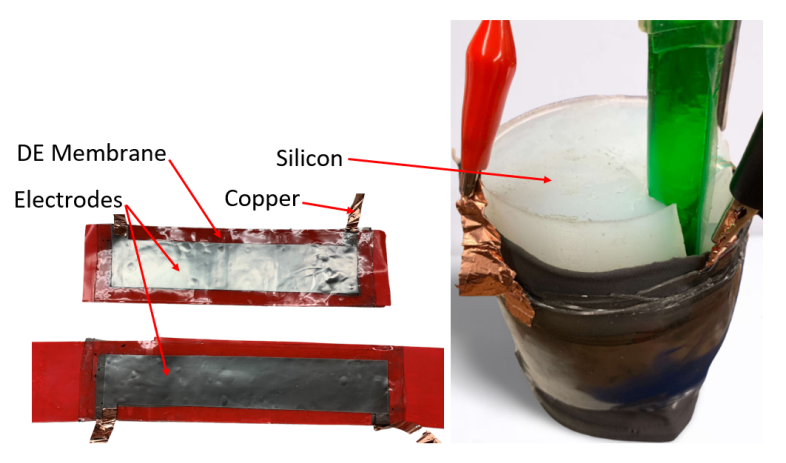


Figure 3: DE strip fabrication(a) and application to simulated muscle-artery setup(b).

The liquid was then re-poured into the plastic casing through the rubber tube using a fluid syringe and then sealed to generate more pressure. A thin wedge was sliced into the rear side of the calf section in order to insert the fluid bag. The fluid bag placement roughly approximates the location of the posterior artery adjacent to the calf muscle. By doing so, the muscle exerts a pressure on the artery. The compression sleeve was then fitted over the silicone muscle, and the DEA stripped was wrapped over the sleeve. (Figure 3b).

#### 3. EXPERIMENTAL SETUP, MODEL IDENTIFICATION, AND VALIDATION

The experimental setup is described in this section. Model identification is performed using the frequency response analysis and validation performed using the time domain data.

#### 3.1 Experiment Setup and Measurement

In Figure 4(a), a syringe is placed at the end of the rubber tube which allows addition of more liquid to increase or reduce the fluid pressure by adjusting the syringe injector. A force sensitive resistor (FSR 402) is used to measure the change in force exerted on the artery. The thin-film sensor is placed between the artery fluid bag and silicone calf simulate. Adjustments are made to ensure a good position to measure the pressure change from the DEA. A 10 k $\Omega$  resistor is selected for the measurement range. A relationship is approximated, using a Matlab curve fitting program, from the data points extracted from the force-voltage curve of the sensor given as

$$F = \frac{(V-c)^{\frac{1}{b}}}{a} \tag{1}$$

where V is the input voltage, a, b, and c are the constants to match the factory calibration curve. The values of the constants are 30.77, 0.02073, and -32.1 respectively. The relationship between sensor resistance, input resistor, and output voltage, as provided by the manufacturer data specifications is

$$V_{out} = \frac{R_M V_{sup}}{R_M + R_{FSR}} \tag{2}$$

where  $R_M$  is the selected 10 k $\Omega$  resistor,  $V_{sup}$  is the 5 V power supply, and  $R_{FSR}$  is the variable force sensor resistance. The voltage applied to the DEA and force change measurement is captured using dSPACE (DS1104) R&D Controller Board. Simulink is used to provide the actuation voltage and to capture output signals. An overview of the system setup is shown in Figure 4(b).

The voltage to the DEA was provided using a sinusoidal input signal. In the first experiment, the peak voltage in the input signal was ranged from 10 kV to 17.5 kV for six different trials with an input frequency of 0.5 Hz. The pressure change was noticeable in the fluid level change observed in the capillary tube as seen with actuation at 17.5 kV show in Figure 5. The nonlinear behavior, delayed response of the DEA is noticed as seen starting

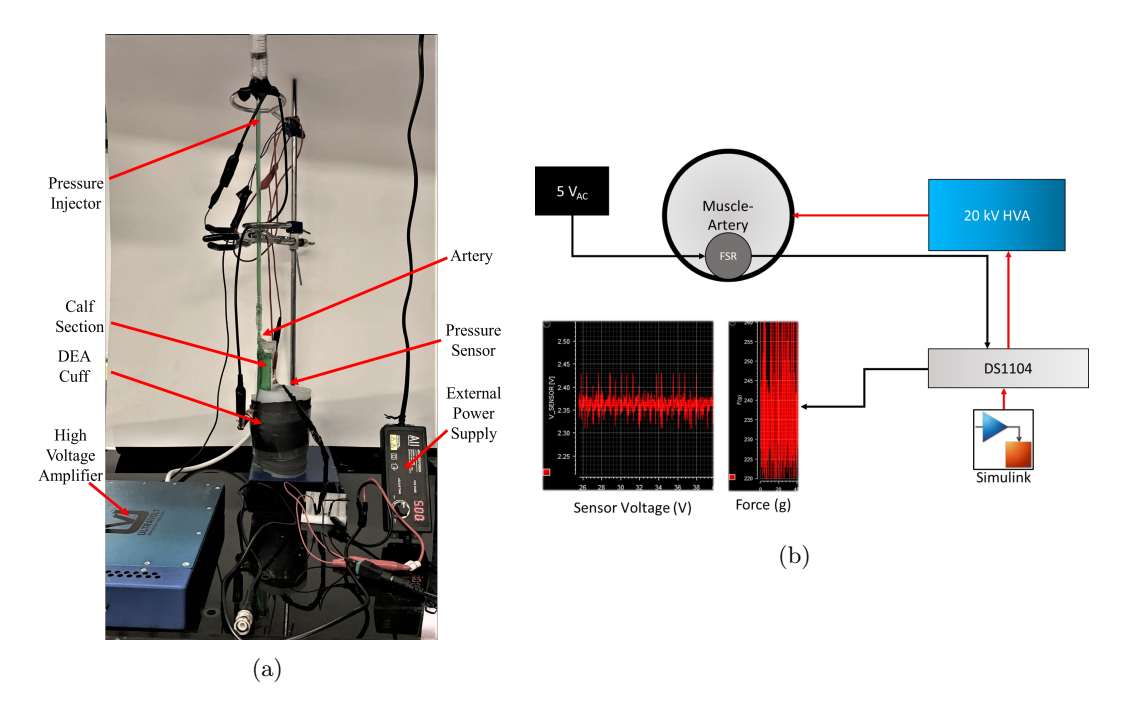


Figure 4: (a) Experiment setup, (b) Layout and interface.

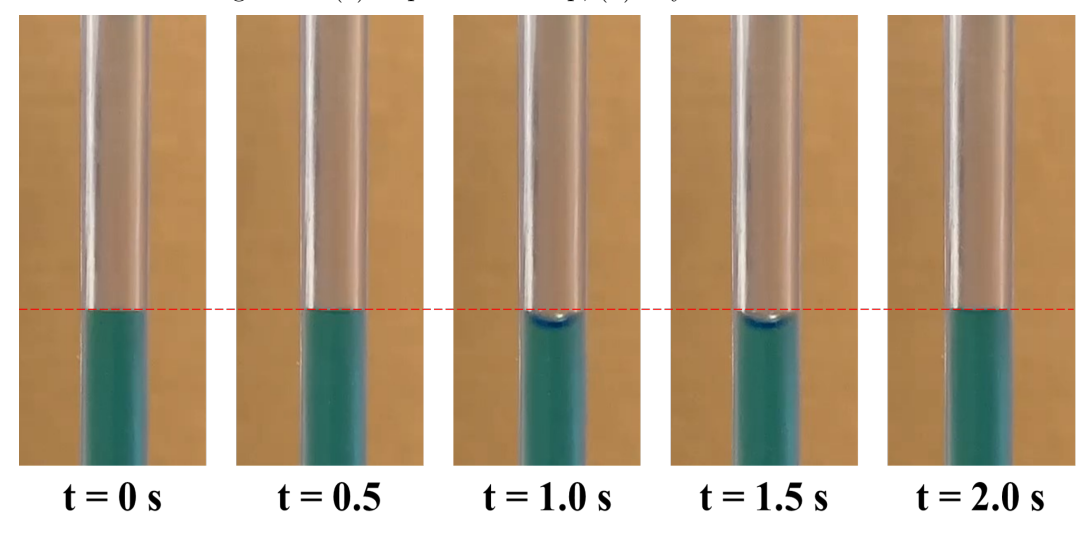


Figure 5: One cycle of the DEA cuff actuation observed in capillary action.

from the third video still frame. The force generated by the DEA around the simulated artery-muscle apparatus produced capillary action inside the artery through the process of relaxation and compression which increases the contact angle at the meniscus of the fluid in the tube. The contact angle increased as the voltage input increased. A relationship between the input voltage and the pressure was observed which has been tabulated below in Table 1. The pressure at zero contact angle was assumed to be the unactuated pressure.

In the second experiment, frequency response analysis is performed with a voltage amplitude of 17.5 kV. The frequency range analyzed is from 0.01 Hz to 6.00 Hz. This range is chosen to include the normal operating range of the heart beat of an adult which is 40 - 120 beats per minute (bpm). This is approximately 0.6 Hz to 2 Hz.

Voltage (kV)	$\theta_c \; (\mathrm{deg})$	$P_{ heta_c}$ (Pa)	ΔP (Pa)
0	0	39.22	0
10	30	33.97	5.255
11	32	33.26	5.960
12	33	32.89	6.328
13	36	31.73	7.491
15	38	30.91	8.314
17.5	40	30.05	9.176

Table 1: Change in gauge pressure,  $P_0=39.22~\mathrm{Pa}$ 

#### 3.2 System Identification and Model Validation

It is expected that the peak-to-peak pressure change decreases as the frequency of the input signal increases. Ideally, the operating point, the unactuated pressure, should remain constant for all trials assuming that there are no other internal factors such as creep. However the change in operating point shows otherwise. As the frequency was increased with each experiment, the experiment became more unstable. The maximum pressure change occurred at 0.001 Hz which was the lowest frequency used for this experiment. Using the area of the DEA, which is  $0.0195 \, m^2$ , the change in pressure was determined to be at most approximately 45.16 Pa which represents a 39.7% change compared to referenced literature. Note that fluid pressure was not taking into account for this experiment, and that the compression sleeve did not contribute significant pressure to the scaled-down lower-limb section. Assuming a linear scaling factor, the pressure change contributed by the DEA cuff would be approximately 101.61 Pa for an typical size calf section. A frequency response analysis for the experimental data and the estimated models is plotted in Figure 6.

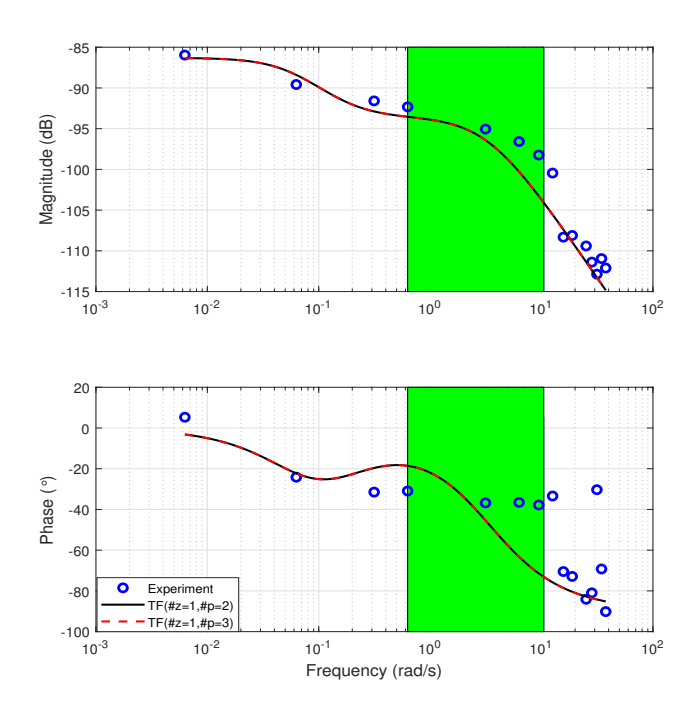


Figure 6: Frequency response of the experiment and the fitted models with the human pulse region highlighted in green.

The fitted curve was determined using the Matlab System Identification feature. A time step of 0.00001 seconds was used. The number of poles and zeros were varied to obtain the best fit. It was determined that a second-order fit (2 poles, 1 zero) and third-order fit (3 poles, 1 zero) produced equivalent fits to the experiment (61.72% fit). From first glance, it seems that system order can be reduced. However, DEAs are considered a third-order system because of its electromechanical behavior, that is, a DEA can be approximated as a spring-mass-damper and RC circuit. Therefore, more data is required to differentiate system order. The data confirmed that the force would decrease with increasing frequency. The data also shows inconsistency at higher frequency. This is a result of the sensor's sensitivity limitation to small measurement changes as well as increase resistance to actuation due to the DEA material properties. Higher frequencies can be ignored since the DE cuff focuses to regulate blood flow within the normal range of the human pulse. This region is highlighted in the Bode plot. The following are approximated transfer functions for the second-order (Eq.3) and third-order system (Eq.4).

$$G_1(s) = \frac{6.853(10^{-5})s + 1.056(10^{-5})}{s^2 + 3.342s + 0.2182}$$
(3)

$$G_2(s) = \frac{1.501(10^5)s + 2.314(10^4)}{s^3 + 2.19(10^9)s^2 + 7.32(10^9)s + 4.779(10^8)}$$
(4)

A time domain representation of the system is additionally used to validate the system order as well as to determine how good of a fit the transfer function is to the experiment. The empirical model was simulated and compared to the experiments. The results are shown in Figure 7.

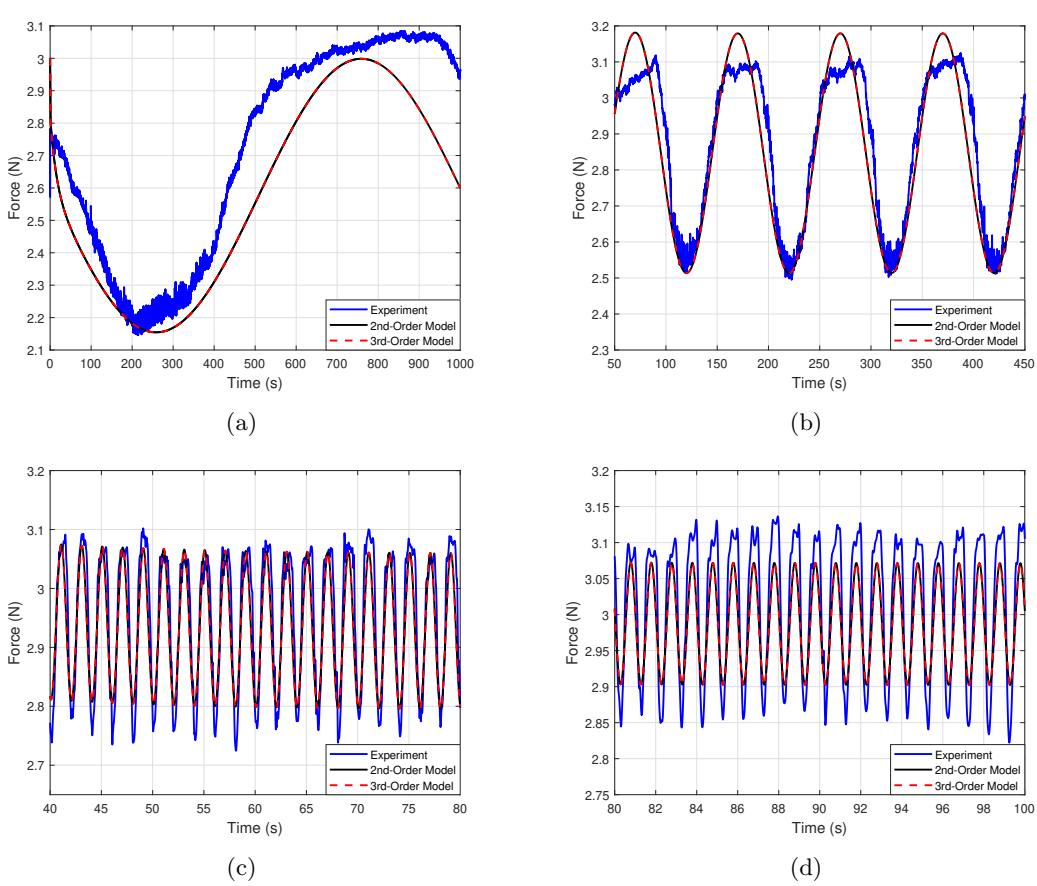


Figure 7: Simulation of estimated system model and experiment at f = 0.001 Hz (a), f = 0.01 Hz (b), f = 0.50 Hz (c), and f = 1.00 Hz (d).

The simulation shows adequate approximation to the experimental results for lower frequency actuation. However, the model assumes that DEAs exhibit pure sinusoidal behavior, which is not the case. Since the actuator is driven by voltage on its electrodes, it is assumed the actuator's circuit structure can be approximated by a classic resistor-capacitor (RC) circuit.<sup>17</sup> For this experiment we can assume the DEA behavior is approximated by a second-order system for simplicity.

Increasing actuation frequency, decreases the change in force (and therefore pressure). The results lead to three known outcomes: (1) As frequency goes to infinity, the change in pressure will be zero. In other words, infinite frequency is equal to the unactuated state in which total pressure is maximum. (2) The DEA will break or will continue to operate with the provided voltage input. (3) Viscoelastic effects (damping) will dominate at high frequency actuation. Similar to the inconsistency seen in the frequency analysis, sensor capability limit a precise measurement for small changes.

#### 4. CONCLUSION AND FUTURE WORK

In this paper, a DEA cuff was designed, fabricated, and tested to demonstrate the feasibility of dynamic actuation. A physical model was used to determine total pressure change due to cuff system as a function of voltage. The results from the experiment provide a framework to further improvement of simulating the DEA cuff physics. This work can be further extended to high frequency regimes to approximate pulse signals equivalent to the human body. Further development of the cuff device will include self-sensing capability in order to measure pressure and pulse signal of the user as well as provide necessary actuation for blood pressure regulation. An H-infinity controller for the physical system can be a suitable controller for tracking human pulse signals. This effort would provide a more natural signal that mimics biological rhythmic patterns enabling future work towards the effort of artificial muscle design.

Experimental refinement is also an integral part of improving the results. A pressure sensor with higher sensitivity should have the capability to capture small pressure changes at high frequency actuation. Measurement location will also improve a more precise pressure measurement in respect to the human anatomy of the lower limbs sections. Successful reproduction or improvement of results can be contributed by improving DEA fabrication. Improving fabrication techniques will increase DEA compliant structural behavior and deformation, allowing for more actuation output with perhaps reduction in applied voltage. Most importantly, performing an experiment at a normal scale should be able to provide a greater magnitude of pressure change. It would be ideal to understand minimum pressure change requirement need to generate sufficient and measurable change to blood flow.

#### 5. ACKNOWLEDGMENTS

This work was supported by the National Science Foundation under Grant CMMI #1747855.

#### REFERENCES

- [1] Mehler, R. E., [How the circulatory system works], John Wiley & Sons (2014).
- [2] Klabunde, R., [Cardiovascular physiology concepts], Lippincott Williams & Wilkins (2011).
- [3] Olufsen, M. S., Ottesen, J. T., Tran, H. T., Ellwein, L. M., Lipsitz, L. A., and Novak, V., "Blood pressure and blood flow variation during postural change from sitting to standing: model development and validation," *Journal of applied physiology* **99**(4), 1523–1537 (2005).
- [4] Cameron, J. L. and Cameron, A. M., [Current surgical therapy E-book], Elsevier Health Sciences (2013).
- [5] Schultheis, L., "The mechanical control system of bone in weightless spaceflight and in aging," *Experimental gerontology* **26**(2-3), 203–214 (1991).
- [6] Brignole, M. and Benditt, D. G., "Orthostatic intolerance: orthostatic hypotension and postural orthostatic tachycardia syndrome," in [Syncope], 179–197, Springer (2011).
- [7] Pei, Q., Rosenthal, M. A., Pelrine, R., Stanford, S., and Kornbluh, R. D., "Multifunctional electroelastomer roll actuators and their application for biomimetic walking robots," in [Smart Structures and Materials 2003: Electroactive Polymer Actuators and Devices (EAPAD)], 5051, 281–290, International Society for Optics and Photonics (2003).

- [8] Ye, Z. and Chen, Z., "Modeling and control of a 2-dof dielectric elastomer diaphragm actuator," *IEEE/ASME Transactions on Mechatronics* **24**(1), 218–227 (2019).
- [9] Duduta, M., Hajiesmaili, E., Zhao, H., Wood, R. J., and Clarke, D. R., "Realizing the potential of dielectric elastomer artificial muscles," *Proceedings of the National Academy of Sciences* **116**(7), 2476–2481 (2019).
- [10] Kovacs, G., Düring, L., Michel, S., and Terrasi, G., "Stacked dielectric elastomer actuator for tensile force transmission," Sensors and actuators A: Physical 155(2), 299–307 (2009).
- [11] Pourazadi, S., Ahmadi, S., and Menon, C., "Towards the development of active compression bandages using dielectric elastomer actuators," *Smart Materials and Structures* **23**(6), 065007 (2014).
- [12] Edher, H., Maupas, L., Nijjer, S., and Salehian, A., "Utilizing tension reduction in a dielectric elastomer actuator to produce compression for physiological application," *Journal of Intelligent Material Systems and Structures* **29**(5), 998–1011 (2018).
- [13] Zhao, H., Hussain, A. M., Duduta, M., Vogt, D. M., Wood, R. J., and Clarke, D. R., "Compact dielectric elastomer linear actuators," *Advanced Functional Materials* 28(42), 1804328 (2018).
- [14] Kaaya, T., Wang, S., Cescon, M., and Chen, Z., "A physics-based and control-oriented model for dielectric elastomer tubular actuator," in [2021 American Control Conference (ACC)], 4472–4477 (2021).
- [15] Mason, J. W., Ramseth, D. J., Chanter, D. O., Moon, T. E., Goodman, D. B., and Mendzelevski, B., "Electrocardiographic reference ranges derived from 79,743 ambulatory subjects," *Journal of Electrocardiology* **40**(3), 228–234.e8 (2007).
- [16] Chang, H., Chen, J., and Liu, Y., "Micro-piezoelectric pulse diagnoser and frequency domain analysis of human pulse signals," *Journal of Traditional Chinese Medical Sciences* 5(1), 35–42 (2018).
- [17] Ye, Z., Chen, Z., Asmatulu, R., and Chan, H., "Robust control of dielectric elastomer diaphragm actuator for human pulse signal tracking," *Smart Materials and Structures* **26**(8), 085043 (2017).